MICROMACHINED PIEZOELECTRIC ULTRASONIC TRANSDUCERS BASED ON PARYLENE DIAPHRAGM IN SILICON SUBSTRATE

Cheol-Hyun Han and Eun Sok Kim*
Department of Electrical Engineering, University of Hawaii at Manoa, Honolulu, HI 96822
*Department of EE-Electrophysics, University of Southern California, Los Angeles, CA 90089-0271

Abstract — This paper describes the fabrication and characterization of a micromachined ultrasonic airborne transducer built on a 1 μm thick parylene polymer diaphragm (flat 5000 * 5000 μm^2 square diaphragm) with electrodes and a piezoelectric ZnO film in a silicon substrate. The sound pressure level at 20 mm away from the fabricated transducer is measured to be around 0.44 Pa at 32.9 kHz (the transducer is driven by a 11 V_{rms} sinusoidal source and measured with B&K 4135 microphone). The vibration amplitude is measured (with a laser Doppler meter) to be about 1 μm at 32.9kHz. Finite element analysis with ANSYS 5.6 has been performed to analyze the static and dynamic behaviors of the transducer under both pressure and voltage loadings.

I. INTRODUCTION

Recently, silicon micromachining technology has been explored to fabricate various ultrasonic transducers due to the following advantages: potentially low cost due to the batch processing nature, possibility of integrating transducers and circuits on a single chip, size miniaturization and low sensitivity to vibration due to small diaphragm mass [1,2]. For a micromachined piezoelectric ultrasonic transducer, we employ a parylene as a diaphragm material, because parylene (a polymer material) has about 50 to 100 times smaller elastic modulus than conventional diaphragm materials such as silicon nitride, polysilicon and silicon. Also, a parylene diaphragm effectively releases the residual stress (in the transducer diaphragm) which is a dominant factor affecting the performance of micromachined, diaphragm-based transducers. Thus, with a proper design, the ultrasonic transducer using parylene as a support diaphragm is expected to have higher acoustic sensitivity and responsivity than the one using silicon nitride diaphragm. Moreover, parylene is an excellent moisture-blocking layer, chemically inert, and biocompatible in many aspects.

This paper describes the techniques used in fabricating the transducers, their performance characteristics, and finite element analyses (FEA) with ANSYS 5.6. With ANSYS, we have calculated the stress and strain (under a static pressure load) and the dynamic mode shapes over a certain frequency range. Also, with appropriate piezoelectric matrices incorporated into the ANSYS batch model, a piezoelectric coupled-field analysis has been performed.

II. FABRICATION

Figure 1 shows the parylene-diaphragm ultrasonic transducer with electrodes and a piezoelectric ZnO film. The key idea in fabricating the parylene-diaphragm (which has relatively low melting point) transducer is the usage of a silicon nitride layer as a temporary structural layer during high temperature process steps. The silicon nitride is removed after completing all high temperature steps and a parylene deposition as shown in Step 10 in Fig. 2.

The fabrication process flow illustrated in Fig. 2 is described as follows. First, 0.5 μm thick low stress silicon nitride is deposited by low pressure chemical vapor deposition (LPCVD) on a bare silicon as a temporary structural layer. After 0.5 μm thick bottom Al is deposited and patterned, 0.5 μm thick piezoelectric ZnO film is sputter-deposited at 275 °C, followed by depositions of 0.2 μm thick parylene as insulating layer, and 0.5 μm thick top Al. After patterning the top Al, we deposit 1 μm thick parylene for the diaphragm support layer, and then open contact holes for access to the bottom and top electrodes. In order to release the diaphragm structure, the silicon nitride on the wafer backside is patterned into a square opening, and the bulk of the

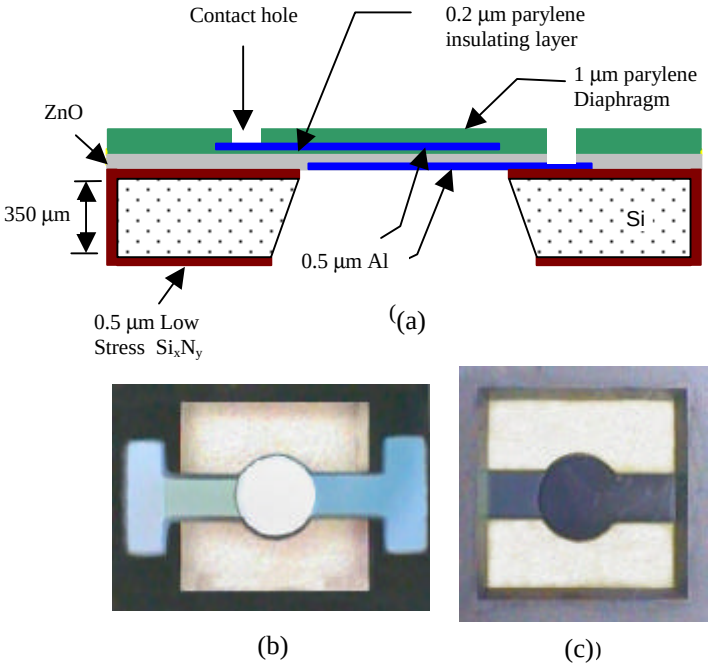

Figure 1 (a) Cross-sectional view of the parylene diaphragm piezoelectric ultrasonic transducer. (b) Top view photo of a fabricated ultrasonic transducer. (c) Bottom view photo of the same transducer.

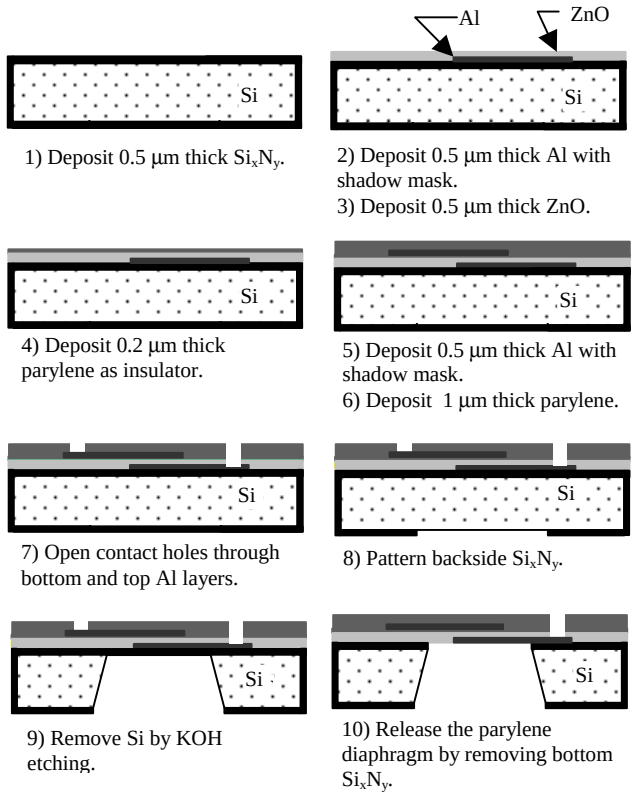

Figure 2 Processing steps to fabricate the parylene flat-diaphragm piezoelectric acoustic transducer.

Figure 3 Photos showing the wrinkled diaphragm due to the compressive stress of the SiN temporary layer. After the SiN is removed from the backside, the diaphragm becomes flat as shown in Fig. 1 (b) and (c).

silicon is removed by KOH from the wafer backside. Finally, the silicon-nitride temporary structure layer is removed from the backside by a reactive ion etcher (RIE) without any etch mask to release the parylene diaphragm.

III. PERFORMANCE OF TRANSDUCER

Figure 3 shows the wrinkled diaphragm of a fabricated transducer (just before the final step of the SiN removal) due to the compressive stress in the SiN temporary layer. After removing the SiN from the backside of the device, the diaphragm becomes flat as shown in Fig. 1 (b) and (c).

To demonstrate the effectiveness of a parylene diaphragm for an ultrasonic acoustic transducer, we have fabricated a conventional SiN diaphragm

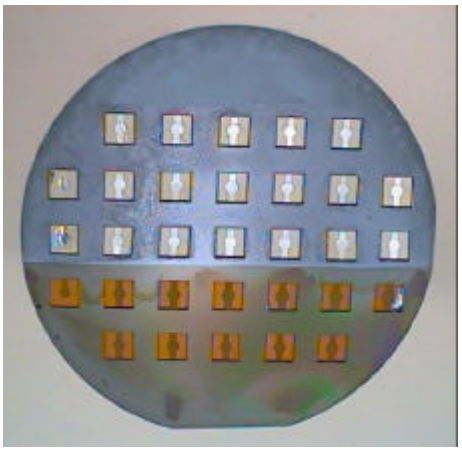

Figure 4 Photo taken from the backsides of a completed 3” silicon wafer that contains both parylene (upper transparent diaphragms) and SiN (lower yellowish diaphragms) piezoelectric acoustic transducers.

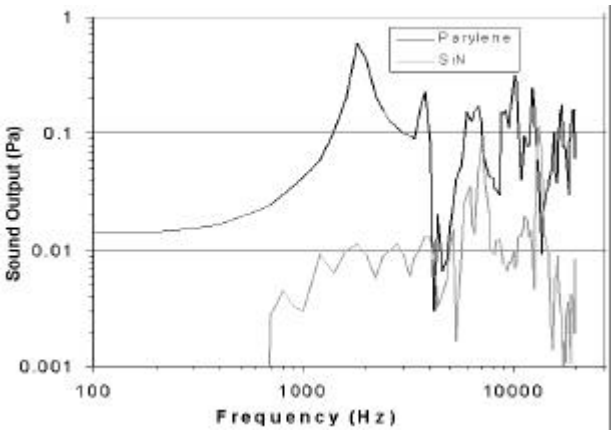

Figure 5 The sound output pressures of the parylene and SiN diaphragm transducers in 100 Hz – 20 kHz range when the transducer is driven by a 11 V_{rms} sinusoidal source and measured with B&K 4135 reference microphone at 2 mm from the transducers.

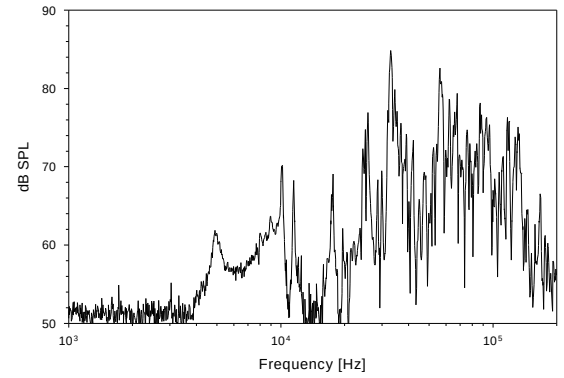

(a)

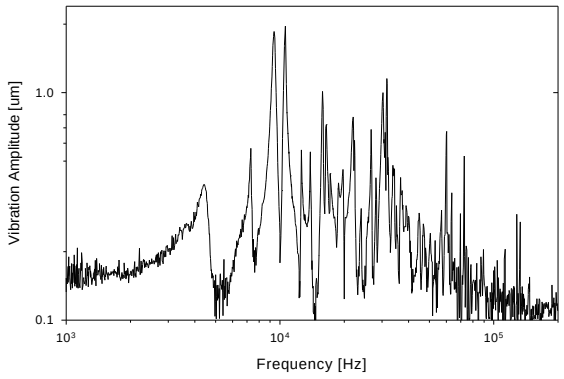

(b)

Figure 6 Measured sound pressure output (20 mm away from the transducer) and diaphragm-vibration amplitude of a packaged parylene microspeaker as a function of frequency in 1 – 200 kHz range when the speaker is driven by a 11 V_{rms} sinusoidal source.

transducer on a same wafer with the same materials, following the same fabrication steps except the diaphragm materials. Figure 4 shows the photo taken from the backside of a completed 3" silicon wafer that contains both the parylene devices (the top three rows) and the SiN devices (the remaining two rows). The sound outputs produced by the parylene-diaphragm transducer and the SiN-diaphragm transducer are compared in Fig. 5. The maximum sound output from the parylene-diaphragm transducer is measured to be 0.6 Pa at the resonant frequency (when the transducer is driven by a 11 V_{rms} sinusoidal source and measured with B&K 4135 microphone 2 mm away from the transducer).

Figure 6 shows the vibration amplitude and sound pressure level (SPL) of the parylene diaphragm transducer in the frequency range of 1 – 200 kHz. At 20 mm away from the parylene diaphragm transducer, we observe a maximum sound output up to 82 dB SPL at 32.9 kHz. Notice that the vibration amplitude at this frequency is not maximum though the sound output is maximum, because sound pressure is proportional to Af^2 where A and f are the vibration amplitude and frequency, respectively.

IV. FINITE ELEMENT ANALYSES

Finite element modeling with ANSYS5.6 software has been performed to study the mechanical behavior of the parylene-diaphragm acoustic transducers. Static analyses for a 1 Pa pressure load and for a 16V-voltage load have been performed. Dynamic mode shape of the diaphragm also has been investigated.

We simplify the model by ignoring the silicon substrate and modeling the parylene diaphragm with a fixed boundary condition, since the vibration of the

Table 1 Material properties used in ANSYS analyses.

Material	Thickness [μm]	Material Properties (Young's Modulus, Poisson's Ratio, Density)
Al	0.5	E=69Gpa, 0.33, 2700kg/m^3
Parylene	0.2, 1	E=3.2 GPa, 0.4, 1289 kg/m3
ZnO	0.5	C11=210 GPa, C12=120 GPa, C13=105 GPa, C33=210 GPa, C44=43 GPa, d=5700 kg/m3
Six Ny	0.5	E=272 GPa, 0.25, 3100 kg/m3

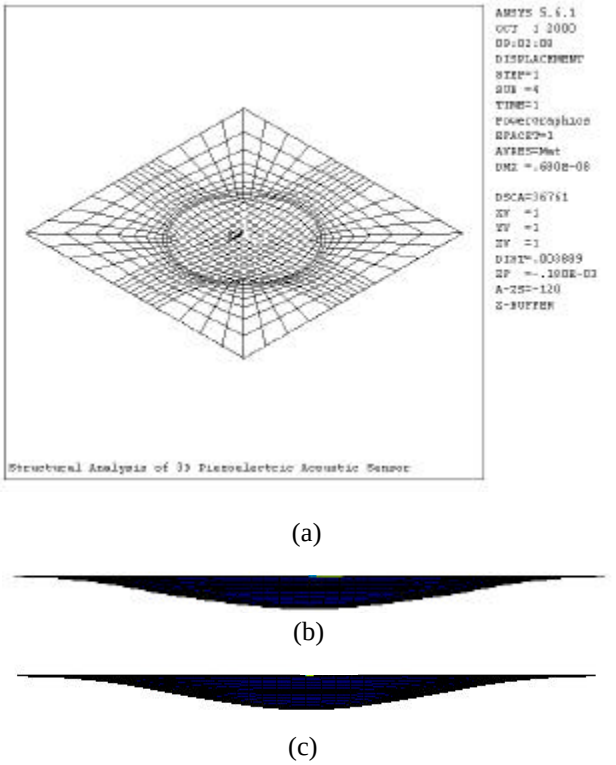

Figure 7 The isometric view (a), side view along the x-direction (b), and side view along the y-direction (c) of the transducer diaphragm under a 1 Pa lateral pressure load.

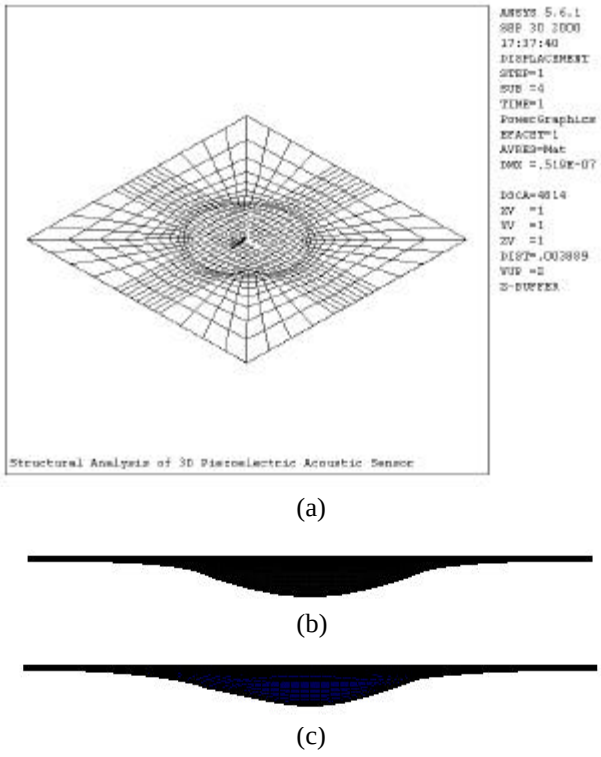

Figure 8 The isometric view (a), side view along the x-direction (b), and side view along the y-direction (c) of the transducer diaphragm under a 16V-voltage load applied to the piezoelectric ZnO layer.

silicon substrate can be ignored due to its large rigidity and thickness of the silicon substrate with respect to those of the diaphragm. The element type of SOLID 185 (that uses eight nodes having three degree of freedom at each node) is used for modeling the mechanical layers such as aluminum and parylene films, while the piezoelectric ZnO layer is modeled with SOLID 5. The SOLID 5 has a three-dimensional piezoelectric and structural field capability with limited coupling between the fields [3]. Table 1 lists the material properties (used in the analysis) from literatures.

Static analysis has been performed to obtain the stress distribution in the transducer diaphragm with its four edges clamped under a lateral pressure load. Figure 7 shows the isometric view and the side views along the x- and y-directions of a deformed diaphragm when a 1 Pa pressure load is applied normal to the diaphragm surface.

Also, static coupled field analysis (between electric and elastic field) for the piezoelectric transducer has been performed with SOLID 5 (a 3 dimensional coupled-field solid). And we have simulated the amount of stress and its distribution when a voltage load (16V on the top electrode and 0V on the bottom electrode) is applied. As can be seen in Figs. 7 and 8, the circular active area of the transducer diaphragm under a voltage load (actuating mode) is deformed to a proportionately larger degree (with respect to the peripheral non-active area) than that of the diaphragm under a pressure load (sensing mode).

Modal analysis has been performed on the transducers to determine the vibration characteristics such as natural frequencies and mode shapes. The Block Lanczos method has been chosen to solve the eigenvalue problem. Figure 9 shows the typical results for the first (a) and second (b) modes of the resonance. The first mode shape shows the symmetric up-and–down mode in which the maximum deflection amplitude (also the maximum-sound output) is at 30.6 kHz. The second mode has a kind of tiling shape at 52.2 kHz.

V. SUMMARY

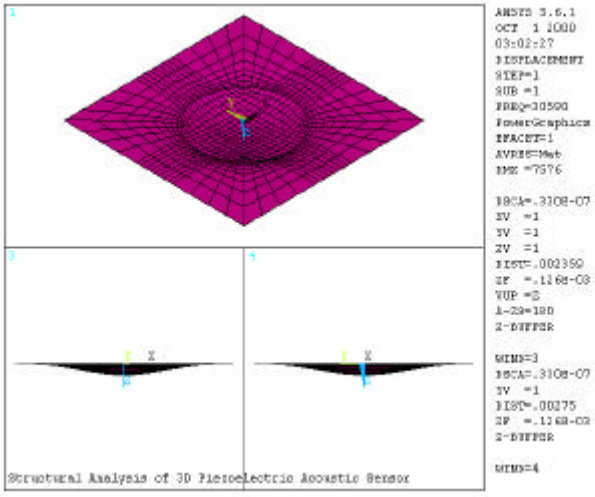

(a)

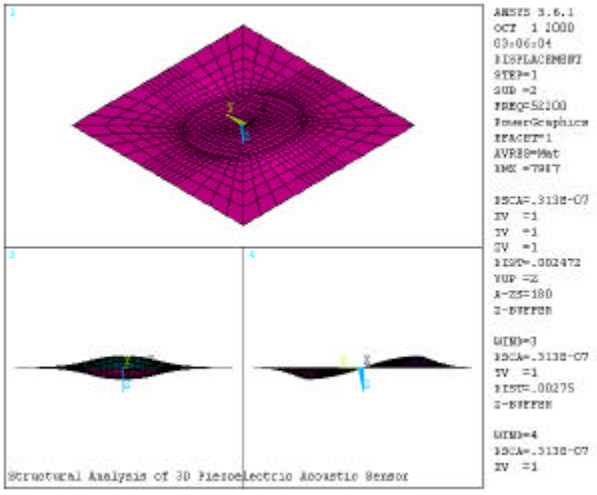

(b)

Figure 9 Typical results of the modal analysis for the first (a) and second (b) modes of the resonance for the parylene diaphragm transducer. Three-different views (isometric view and side views along the x- and y-directions) are shown for clarity.

We have successfully fabricated piezoelectric acoustic transducers built on a 1 μm thick parylene diaphragms (5,000*5,000 μm^2 square diaphragm on a silicon substrate) with electrodes and piezoelectric ZnO film. The sound pressure level at 20 mm away from the parylene diaphragm transducer is measured to be around 0.44 Pa at 32.9 kHz (the transducer is driven by a 11 V_{rms} sinusoidal source and measured with B&K 4135 microphone). The vibration amplitude is also measured as a function of frequency with a laser Doppler meter, and is about 1 μm at 32.9 kHz. Finite element analyses with ANSYS5.6 have been performed to study the static and dynamic behaviors of the micromachined parylene-diaphragm acoustic transducers, and some results are presented in this paper.

VI. ACKNOWLEDGMENTS

This material is based upon work supported by Naval EOD Technology Division under contract N00174-98-K-0016.

VII. REFERENCES

[1] Oliver Brand, Mark Hornung, Henry Baltes, and Claude Hafner, "Ultrasound Barrier Microsystem for Object Detection Based on Micromachined Transducer Elements," Journal of microelectromechanical systems, Vol. 6, No. 2, pp. 151-160, June 1997

[2] David W. Schindel, David A. Hutchins, Lichun Zou, and Michael Sayer, "The Design and Characterization of Micromachined Air-Coupled Capacitance Transducers," IEEE Transactions on ultrasonics, ferroelectrics, and frequency control, vol. 42, No. 1, pp. 42-50, January 1995.

[3] ANSYS Release 5.6 User Manuals, 1999